

REPORT DOCUMENTATION PAGE

AFRL-SR-BL-TR-99-

0271

Public reporting burden for this collection of information is estimated to average 1 hour per response, including the time for reviewing instructions, searching existing data sources, gathering the required data, reviewing the collection of information, Send comments regarding this burden estimate or any other aspect of this collection of information, including suggestions for reducing the burden, to Washington Headquarters Services, Directorate for Information Operations and Reports, 1215 Jefferson Davis Highway, Suite 1204, Arlington, VA 22202-4302, and to the Office of Management and Budget, Paperwork Project, Washington, DC 20503.

ing and reviewing
s for information

1. AGENCY USE ONLY (Leave blank)		2. REPORT DATE 26 October 1999	3. REPORT TYPE AND DATES COVERED Final Technical Report 01 Aug 98 to 31 Jul 99
4. TITLE AND SUBTITLE Novel Mathematical/Computational Approaches to Surveillance Image Transmission and Exploitation			5. FUNDING NUMBERS F49620-98-C-0036
6. AUTHOR(S) Dr. Charles Hsu			
7. PERFORMING ORGANIZATION NAME(S) AND ADDRESS(ES) Trident Systems Inc 10201 Lee Highway Suite #300 Fairfax, VA 22030			8. PERFORMING ORGANIZATION REPORT NUMBER
9. SPONSORING/MONITORING AGENCY NAME(S) AND ADDRESS(ES) AFOSR/NM 801 N. Randolph Street, Rm 732 Arlington, VA 22203-1977			10. SPONSORING/MONITORING AGENCY REPORT NUMBER F49620-98-C-0036
11. SUPPLEMENTARY NOTES			
12a. DISTRIBUTION AVAILABILITY STATEMENT Approved for Public Release; Distribution Unlimited.			12b. DISTRIBUTION CODE
13. ABSTRACT (Maximum 200 words) Current image compression algorithms are founded on three basic principles: transformation, quantization, and entropy coding. The transformation attempts to remove statistical redundancies from the input, thereby reducing the data to a smaller, more manageable set. The process of quantization converts samples into a finite set of levels, typically in a way that minimizes some predefined error measure (e.g. mean-squared, mean absolute difference, etc.). The entropy coder converts the quantized output, which is in the form of a sequence of level values, into a bit string. Assignments are made with variable length codes in an attempt to minimize the overall average bit rate of the system.			
14. SUBJECT TERMS			15. NUMBER OF PAGES 32
			16. PRICE CODE
17. SECURITY CLASSIFICATION OF REPORT Unclassified	18. SECURITY CLASSIFICATION OF THIS PAGE Unclassified	19. SECURITY CLASSIFICATION OF ABSTRACT Unclassified	20. LIMITATION OF ABSTRACT UL

19991130 033

**Final Technical Report
for
SBIR Phase I
Contract F49620-98-C-0036
AF98-009 STTR**

***(Novel Mathematical/Computational Approaches to Surveillance
Image Transmission and Exploitation)***

26 October 1999

Submitted to:

**Dr. Jon Sjogren, COTR
AFOSR/NM
Rm 732
Arlington, VA 22203-1977**

Prepared by:

**Trident Systems Inc.
10201 Lee Highway Suite #300
Fairfax, VA 22030
(703) 273-1012**

ABSTRACT

Current image compression algorithms are founded on three basic principles: transformation, quantization, and entropy coding. The transformation attempts to remove statistical redundancies from the input, thereby reducing the data to a smaller, more manageable set. The process of quantization converts samples into a finite set of levels, typically in a way that minimizes some predefined error measure (e.g. mean-squared, mean absolute difference, etc.). The entropy coder converts the quantized output, which is in the form of a sequence of level values, into a bit string. Assignments are made with variable length codes in an attempt to minimize the overall average bit rate of the system.

This study examined and developed image compression codecs. Current compression methodologies such as Joint Photographers Expert Group (JPEG) and others were evaluated in context of Synthetic Aperture Radar (SAR) image compression. Specifically, this benchmarking was performed in terms of visual quality and Automatic Target Recognition (ATR) performance quality. This is in direct contrast to mean-square error (MSE) and peak signal to noise ratio (PSNR) measures that are commonly used to assess image-coding quality in the compression community. This important first step is done in recognition that the true measure of merit for defense applications is the preservation of target classification information after transmission. It was determined that much of the high frequency content found in SAR images was lost due to these compression techniques. Regenerating this speckle by modeling a stochastic process often reduces PSNR and MSE but increase perceptual quality.

Speckle extraction and regeneration techniques were developed, implemented and evaluated on real Joint STARS SAR imagery. Image interpretation experts then analyzed and rated the compressed images.

Table of Contents

1.0	Summary	1
2.0	Introduction	2
3.0	Methods, Assumptions, and Procedures	4
3.1	Structure/Texture Model	4
3.2	Pre/Post Processing Algorithm	6
3.2.1	Pre-Processor Description	7
3.2.2	Post-Processor Description	7
3.3	Region Of Interest	8
3.4	SAR Image Coders	9
3.4.1	Optimized Subband Coder	9
3.4.2	Error Resilient Subband Coder	12
3.4.3	Biorthogonal Wavelet Coder	12
4.0	Results and Discussions	14
4.1	Performance Evaluation	14
4.1.1	Optimized Subband Coder Results	19
4.1.2	Structure-Texture Coder Results	22
4.1.3	Error Resilient Coder Results	26
V.	Conclusions	30
VI.	Future Considerations	31
VII.	References	32

LIST OF FIGURES

- Figure 1: Algorithm Component Block Diagram**
- Figure 2: Structure/Texture Components of Image**
- Figure 3: Wrapper Transmission System Block Diagram**
- Figure 4: Pre-Processor Block Diagram**
- Figure 5: Wrapper Post-Processor Block Diagram**
- Figure 6. ROI Comparison**
- Figure 7. Block diagram of SB-RSQ system**
- Figure 8. Diagram of the inter-stage, inter-band, and intra-band conditioning scheme**
- Figure 9: Performance Comparisons**
- Figure 10: Image Comparisons**
- Figure 11. Pentagon Compressed 8:1 With Optimized Subband Coder**
- Figure 12. Pentagon Compressed 16:1 With Optimized Subband Coder**
- Figure 13. Pentagon Compressed 32:1 With Optimized Subband Coder**
- Figure 14. Pentagon Compressed 64:1 With Optimized Subband Coder**
- Figure 15. Pentagon Compressed 8:1 With Structure Texture Model**
- Figure 16. Pentagon Compressed 16:1 With Structure Texture Model**
- Figure 17. Pentagon Compressed 32:1 With Structure Texture Model**
- Figure 18. Pentagon Compressed 64:1 With Structure Texture Model**
- Figure 19. Original Image**
- Figure 20. SPHIT Image Compressed to 0.25 bpp With a BER of 10^{-4}**
- Figure 21. Error Resilient Image Compressed to 0.25 bpp With a BER of 10^{-4}**

1.0 SUMMARY

Image compression in general exploits the inherent redundancy in the data in order to reduce the overall file size. The types of redundancy are spatial and spectral. Another key aspect, which is often exploited, is the fact that image content, particularly images from visible sensors, is characterized by low frequency information. Coupled with this is the fact that the human visual system (HVS) is very limited in its spatial frequency sensitivity and parts of hence part of the image content can be discarded without any visible loss to the human eye. Most of these aspects are leveraged by image compression algorithm developers to achieve the highest compression ratio possible while still presenting the best quality for the user. SAR imagery is very different than imagery from visible sensors since it contains a wide spatial frequency range of information – i.e. both high frequency and low frequency information content. SAR images are generally characterized by low contrast, with occasional high amplitude bright returns, and an overall speckled appearance caused by the coherent addition of scatterers. The speckle is high frequency in nature and imposes a higher degree of difficulty of processing such as pattern classification and compression. Popular lossy compression techniques are not well suited to SAR data due to the complexity of the image statistics.

In developing an image compression system, it is important to know how and who will be using the data after it is received. This will determine overall compression ratio, desired quality, and specific features to be preserved. An example of this are observed with the imagery requirements of an image analyst compared with a battlefield commander. The imagery analyst will desire very high quality imagery with visible loss of information and preservation of the unique image features such as speckle. In contrast, a battlefield commander is generally only concerned with, for example, is there a column of tanks coming down the road. Given this, the battlefield commander can reasonably accept a certain amount of imagery quality loss and does not necessarily require the preservation of image features such as speckle. For these reasons, it is important to have a compression system that is flexible to be able to meet a wide number of user requirements.

This study concluded that the current standard compression techniques lost too much of the desired high frequency speckle that image analyst desire. Therefore, special algorithms are required for those that desire this speckle. Our structure-texture algorithm combined with standard or newly developed compression techniques provides very good speckle regeneration capabilities while allowing very good compression. Image analysis experts rated the loss of many images compressed 64:1 as being minimal, and acceptable for battlefield personnel. Also, for higher compression ratios, our compression models achieve better performance both perceptually and mathematically compared to discrete cosine transform based algorithms.

More work is needed to improve the performance of these coders. One major consideration must be made to account for channel errors. Since these images will be transmitted in noisy battlefield environments, the codecs must be able to handle numerous bit errors. Also, the code should be optimized to run efficiently on the Joint STARS platform.

2.0 INTRODUCTION

The Trident Systems and Georgia Tech team synthetic aperture radar (SAR) processing effort provides a modular set of algorithms, which are flexible to meet the end users requirements. This suite of algorithms is based on Trident and Georgia Tech's extensive experience with a wide variety of customers in this area. A basic block diagram of the modular algorithm approach is shown in Figure 1.

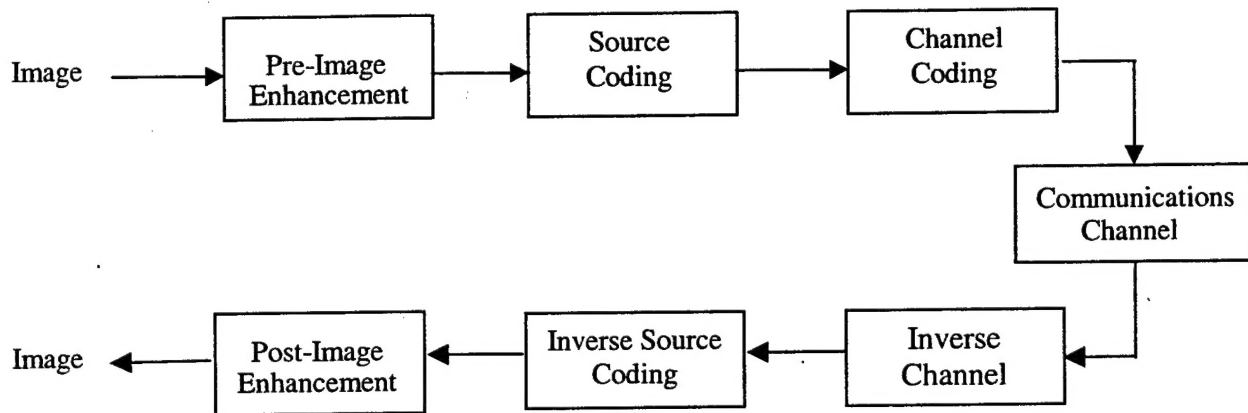


Figure 1: Algorithm Component Block Diagram

The first component of the block diagram is the Pre-Image Enhancement function. This consists of two algorithms – Pre-Processing and Structure/Texture. The Pre-Processing algorithm operates on the image data prior to any source coding and performs two basic functions. The first is to automatically extract and enhance regions of the image which contain more important information content compared to the rest of the image. The second function of this algorithm is to filter or smooth portions of the image that contain less important information content. This Pre-Processing function has been shown to help improve overall compression performance between 10 – 20% while still maintaining overall image quality. The second algorithm for image enhancement is the Structure/Texture. This algorithm preserves the speckle component of the SAR image that often contains critical information and is a desired feature of image analysts. An important feature of these image enhancement algorithms is that they can be used separately, together, and with any compression algorithm.

The second component in the block diagram is the source coding. For this we have two main algorithm approaches – Joint/Source Subband, and Biorthogonal Wavelet Algorithms. The Joint/Source Subband has several unique features. The basic idea of this approach is that the compression system will produce a bit stream which contains two distinct bit sequences which can then be protected differently according to their importance and channel noise considerations. This approach provides robustness against channel noise. It is important to note that this is completely separate from error correction. The Biorthogonal Wavelet algorithm provides performance that is comparable to the Joint/Source Subband but it requires fewer computations though it is not robust against channel noise. It should be noted that the pre-processing function described above can be used with either of the above source coding algorithms.

The third block is the channel coding. We have a complete family of algorithms that include block codes, convolutional codes, turbo codes and channel models that can be used in conjunction with the source coding algorithms. In addition to traditional channel coding algorithms, we have developed an error resilient subband coder. This approach does not try to correct errors when they occur. Instead, it tries to prevent the errors from propagating through the bit stream. It is this propagation of errors that usually renders an image useless when a few, or even a single bit error occurs.

The inverse channel and inverse source coding blocks follow the communications channel in the block diagram. These processes are the counter parts of the channel and source coding components. If no channel errors occur, this part of the process should be loss less.

The final component of the block diagram is the image enhancement component. This consists of the Post-Processing and the speckle synthesis algorithms. The Post-Processing function determines where the important edge information is and tries to enhance these important areas of the imagery. Also, if the image was down sampled by the Pre-Processing function, the Post-Processor will restore the image to the original size. The speckle synthesis algorithm generates speckle by modeling a stochastic function described by the set of transmitted parameters.

3.0 METHODS, ASSUMPTIONS, AND PROCEDURES

3.1 STRUCTURE/TEXTURE MODEL

A focal point of study in this research has been the reduction and attempted removal of speckle in order to improve performance in some applications like automatic target recognition. However removing speckle can also remove information associated with characteristics of the terrain and surroundings of targets. Image analysts are trained to infer the context of a scene that contains targets using the speckle. The remote sensing community relies on the textural characteristics (i.e. speckle) of SAR images to perform studies on vegetation, agriculture, geology, etc. Thus, it is important to preserve both.

In this section we propose a model-based approach in which speckle is considered to be a texture. The Structure Texture coder is specifically tailored to achieve high compression of SAR images with minimal loss of perceptual characteristics. In general, texture can be defined as a quality of the surface that conveys to the observer a feeling of visual uniformity caused by the quasi-periodic repetition of some pattern (s).

To separate the two components, the coder applies subband denoising with a different threshold on each subband. The resulting "denoised" image retains the large objects and structures with minimal loss in edge sharpness. This structural component is coded using a multiresolution-quadtrees coder, which outperforms other coders like SPIHT and JPEG at the lower bit rates. The textural component is obtained by taking the difference of the SAR image and the denoised version. The difference image is parameterized using state of the art speckle models. Two models are available at the moment. The first is a two-dimensional autoregressive model and the second model is based on matching the first order spatial statistics of the subbands from a directional decomposition. The speckle parameter set is compact and only requires a modest fraction of the bit budget. This allows the algorithm to apply most of the bits to the structural component. The decoder takes the speckle parameters and performs speckle synthesis. The synthesized speckle is added to the decoded structure to obtain an image that exhibits the same visual properties as the original.

The image model in this case views a SAR image $X(i,j)$ as the combination of two components: structure $S(i,j)$ and texture $T(i,j)$, and can be represented by

$$X(i, j) = R(S(i, j), T(i, j))$$

where $R()$ is a recombination rule for the two components and is shown pictorially in Figure 2.

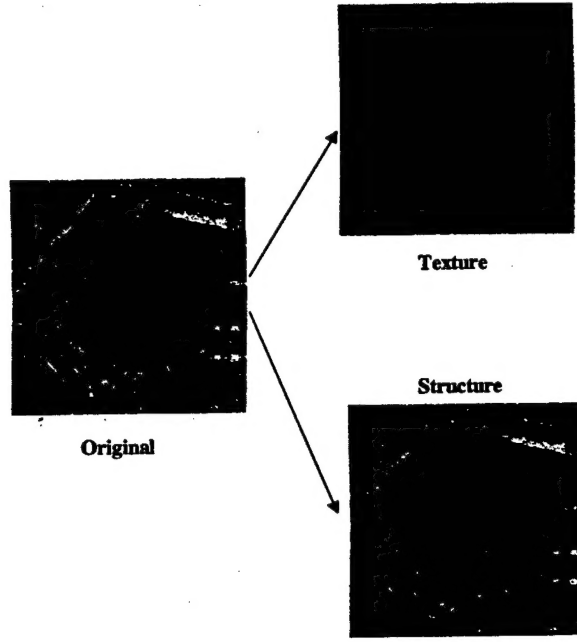


Figure 2: Structure/Texture Components of Image

However, the starting point is the intensity image $X(i,j)$ from which $S(i,j)$ and $T(i,j)$ need to be de-coupled. Speckle information resides mostly in the two finer levels while most of the large patterns, intensity and edge information reside in the remaining coarser levels. Thus, doing only a three level decomposition on $X(i,j)$, we form two sets of wavelet coefficients, X_{SBC}^I and X_{SBC}^{II} where X_{SBC}^I contains the wavelet coefficients of subbands 1,2,3 and 4 (as numbered in Fig. 1(b)) and X_{SBC}^{II} contains the coefficients of the remaining subbands. However, for images with very strong edges, there is still a good amount of edge information in X_{SBC}^{II} . In [10], Servetto, et al. concludes that for natural images, edge information in the subband domain tends to cluster in regions where coefficients have large magnitudes. A nonlinearity given by

$$Q(c) = \begin{cases} 0 & -\alpha * C_{max} < |c| < \alpha * C_{max} \\ c & \text{otherwise} \end{cases}$$

was applied to each subband of X_{SBC}^{II} , where C_{max} is the maximum coefficient magnitude of a subband, c is a coefficient in the given subband and α is a parameter that controls the width of the dead zone. It was found that this operation would retain edge information while eliminating those subband coefficients related to speckle. Two new sets of subband coefficients are then defined as

$$X_{SBC}^{(S)} = X_{SBC}^I \cup Q\{X_{SBC}^{II}\}$$

and

$$X_{SBC}^{(T)} = X_{SBC}^{II} \setminus Q\{X_{SBC}^{II}\}$$

Thus, the recombination rule becomes simple addition of two 2-D fields, where

$$X(i, j) = S(i, j) + T(i, j) = \text{Synthesis}(X_{SBC}^{(S)}) + \text{Synthesis}(X_{SBC}^{(T)})$$

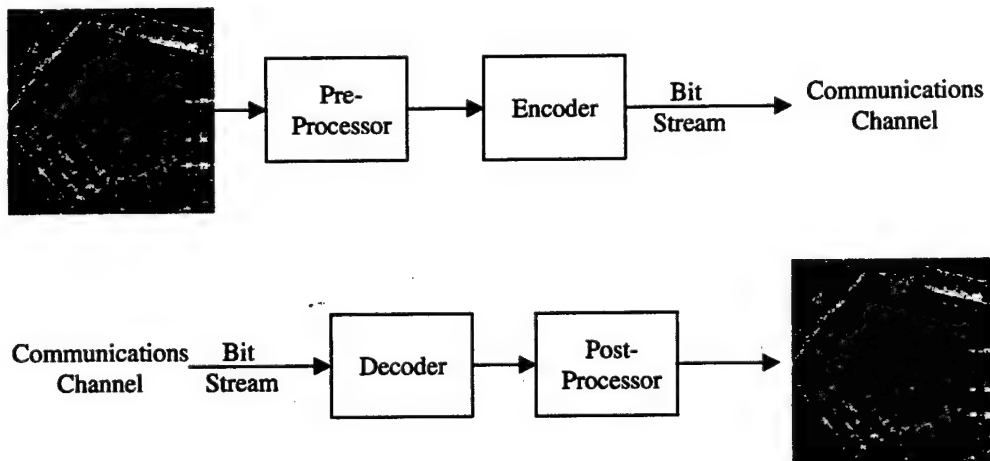
It is important to note that there is a limit to the ability of decoupling the two components. In images where there are very strong edges, (like the ones caused by roads, building, or targets) $T(i, j)$ still preserves edge information. This separation model is considered acceptable for our purposes.

In coding the speckle texture component of the imagery, it can be modeled as a stochastic process that is rich in high frequencies. There are several approaches for modeling and synthesis of the texture component. There are various approaches that have been studied in the literature. These include models based on second order statistics (i.e. co-occurrence matrices), histogram and autocorrelation. It is not guaranteed that the models will work on all textures or produce a manageable parameter set. There are two approaches proposed for this effort – one based on auto-regressive models and the other based on a pyramid decomposition model.

One of the most important aspects of this approach of modeling and coding the texture component is to allow one to use any coder for the structure component of the image. This allows the user to use one of our proposed algorithms or use one of the new emerging standards such as JPEG2000.

3.2 PRE/POST PROCESSING ALGORITHM

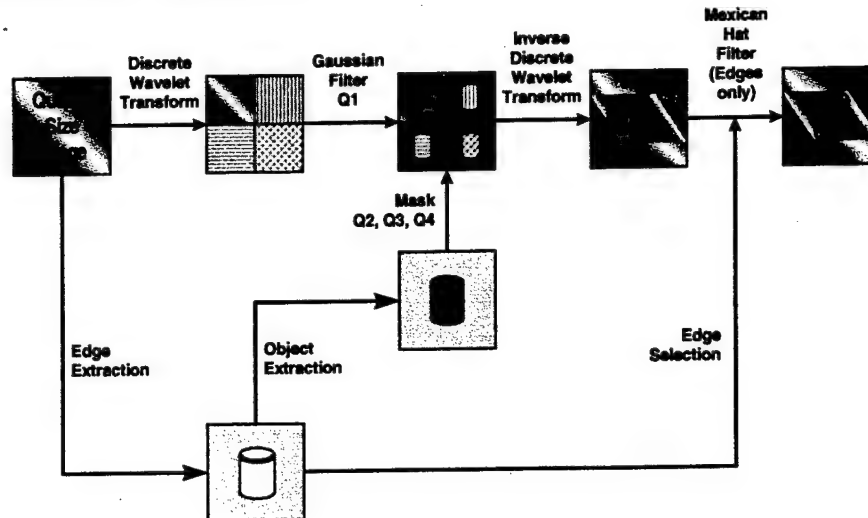
The image wrapper algorithm provides a pre-processor in front of the image encoding process and post processor after the image decoding process. The pre-processor's primary function is to reduce the overall dimensionality of the image frame input to the encoding process. In order to compensate for the reduced dimensionality the algorithm enhances objects within the video frames allowing the CODEC to encode frames with acceptable image quality. The net result of the pre-processor is that encoded frames can be transmitted over a smaller communications bandwidth. The post processor receives the decoded image frames from the CODEC and restores them to the full dimensionality. A simplified block diagram of the transmission system is shown



in Figure 3

Figure 3: Wrapper Transmission System Block Diagram

3.2.1 Pre-Processor Description



The pre-processor increases the compression ratio of the encoder by smoothing the high frequency pixels. The pre-processor includes image size reduction, edge extraction, object extraction, Discrete Wavelet Transform (DWT), Inverse Discrete Wavelet Transform (IDWT), and filtering operations. The pre-processor structure is shown in Figure 4. The major routine processes include the operations of DWT-Filtering-IDWT-Filtering; the edge-extraction and the object-extraction operations are included in the sub-routine process. The algorithm may pre-process any size image. For the application of any encoder, a full size image is captured, decimated to quarter size, and processed by the 1-level DWT. Four different sub-band sub images are obtained after the operation of the 1-level DWT. Then, the objects of the sub images may be defined by edge and object extraction of the original image. The object information is used to apply Gaussian filtering operations in the non-object areas. The IDWT operation is applied to reconstruct the quarter size image. The edge information of the original image is used to apply a Mexican hat filtering function to the reconstructed image adding important information for the image coder.

Figure 4: Pre-Processor Block Diagram

3.2.2 Post-Processor Description

The post-processor de-noises the reconstructed image, increases the edge information, and expands the size of the image. The post-processor includes edge extraction, object extraction, Discrete Wavelet Transform (DWT), Inverse Discrete Wavelet Transform (IDWT), and filtering operations. The post-process algorithm may be applied to any size video image. The structure of the post-processor is shown in Figure 5. The decoded quarter size image is expanded by doubling each pixel in the vertical and the horizontal directions, then applying a 1-level DWT. The first quarter (left upper) of the DWT image is replaced by the original image and an IDWT is applied to obtain a reconstructed image with double the size (2x) of the original image. Then edge extraction is applied to detect edge information and object extraction defines the objects in this reconstructed image. Next, the objects and background are smoothed by using Gaussian filter functions and the edges are enhanced by using a Mexican hat filter function.

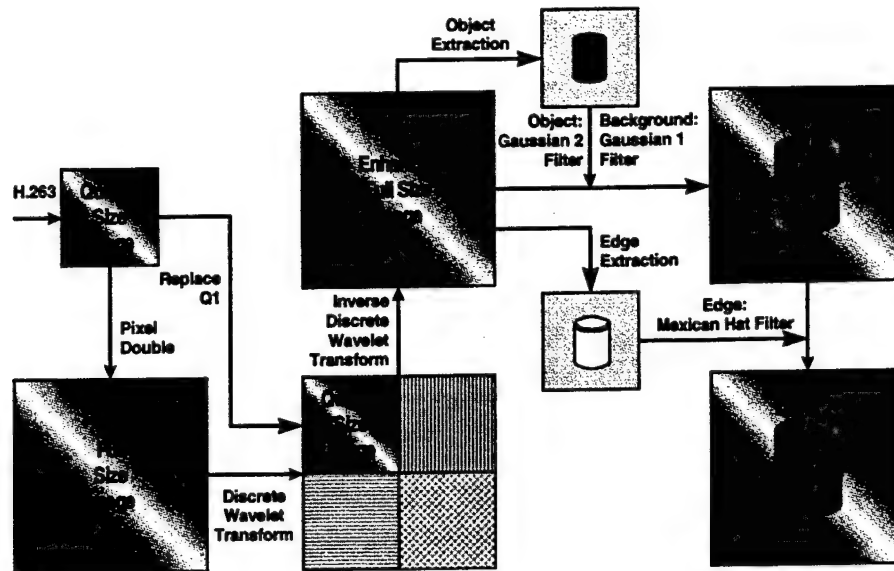


Figure 5: Wrapper Post-Processor Block Diagram

3.3 REGION OF INTEREST

An additional function is the Region of Interest (ROI) algorithm. While this basic concept of ROI is not new, we have developed a unique approach that provides superior performance. Most approaches to ROI simply cut out the ROI, compress at a very low compression ratio such as 2:1 while over compressing the background. The ROI and the background are transmitted separately and put back together on the receiver's end. While this works reasonably well, it results in blocking discontinuities between the ROI and the background that are very displeasing to the human observer. Our approach transforms the entire image and assigns additional bits to the ROI. This coupled with additional processing yields a ROI with the same performance as the "brute force" approach but yields an image which is much more pleasing to the observer. Figure 6 shows the simulation results using wavelet transform for higher compression (left) and region of interest using discrete transform (right). The file size is 1700 bytes for higher compression without region of interest, and 2600 bytes for one with region of interest.

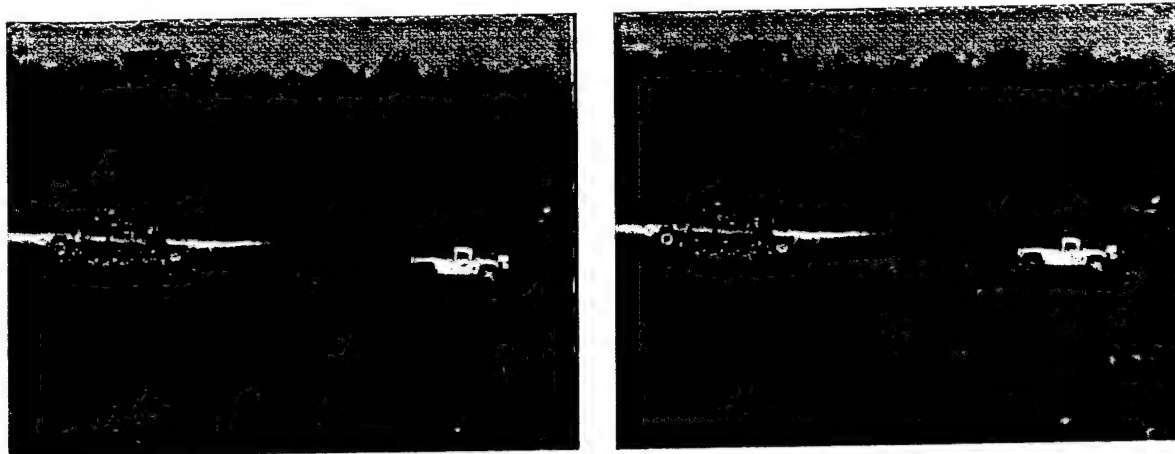


Figure 6. ROI Comparison

3.4 SAR IMAGE CODERS

3.4.1 OPTIMIZED SUBBAND CODER

One of the first ideas that comes to mind when trying to develop a scheme for SAR image compression, is that there could be an improvement if the compression scheme was tailored to the statistical characteristics of the source. A way to achieve this objective is to develop an algorithm that is trained with SAR images and generates an optimal quantization and coding technique. The statistics of SAR image data are markedly different from those of natural images.

This subband coder approach optimizes jointly within and across the subbands in a complexity- and entropy-constrained framework. The algorithm used to design the coder employs multistage residual quantizers that features very low complexity and memory, and provide much greater control over both design and encoding complexity. An important aspect of the algorithm is that no explicit bit allocation is needed. The bits are indirectly (but optimally) allocated among the subbands during the design process. The coder exploits both statistical intra-band and inter-band dependencies simultaneously, mainly through complexity-constrained high-order conditional entropy coding.

The input signal is first decomposed into M subbands using uniform decomposition. Each subband is then encoded using a sequence of P_M residual scalar quantization (RSQ) fixed-length encoders. A block diagram of the coder is depicted in Figure 7. RSQs can provide excellent joint quality and rate control. The output symbol for each stage quantizer is fed into an entropy coder driven by a high-order stage statistical model that is controlled by a finite state machine (FSM), which allows the statistical model to switch among several zero-order conditional models (represented by first order probabilities) based on the state transitions. Finally, the output bits of the entropy coders are combined together and sent to the channel. Since only previously coded symbols are used by the FSM, no side information is necessary and the decoder can track the state of the encoder.

The design algorithm minimizes the expected distortion subject to a constraint on the overall entropy of the product of the M subband quantizers. The design algorithm is an interactive

descent algorithm based on a Lagrangian minimization. Given a fixed Lagrangian parameter X , the algorithm attempts to satisfy simultaneously optimality conditions, requiring the subband encoders, decoders, and entropy coders be designed jointly. The parameter X is chosen based on the overall rate and distortion of the subbands, and is used in the entropy-constrained design of all subband quantizers. Therefore, explicit bit allocation is not needed in the design process.

The complexity and memory associated with the design algorithm grow exponentially as a function of the quantization and entropy coding parameters. To reduce them substantially, constrained quantizers must generally be employed. Multistage residual quantizers are chosen, mainly because they require relatively low encoding complexity and memory, and because they simplify the design process by providing greater control over the complexity-performance tradeoffs.

The most important advantage of the multistage residual structure is that it allows for substantial reduction in the complexity and memory by making the output alphabet of the stage quantizers small (e.g., 2, 3, and 4). Moreover, multistage quantizers provide another dimension to improve the optimization of the coder. To illustrate this point, Figure 4 shows the inter-stage, inter band, intra band conditioning scheme used in the system.

In the design of the entropy codes stage, conditional entropies are used. The conditioning is performed on previously coded pixel values located next to the current pixel, in the corresponding pixel positions across subbands and in corresponding positions across stages, as illustrated in Figure 8. A more detailed description of this algorithm can be found in (1).

For this implementation, all stage codebooks in all subbands contain 3 scalars. The initial maximum allowed number of conditional probabilities N is set to 2048. The output of each of the stage fixed-length RSQ encoders is encoded using an adaptive arithmetic coder by the conditioning model just described.

This approach has been shown to have significant improvement in both visual quality and PSNR when compared to SPIHT and MRWD. The speckle is very well preserved for the 0.50 bpp case; the more noticeable distortion is the loss of high reflector points in the coded images, giving the impression of having lower contrast.

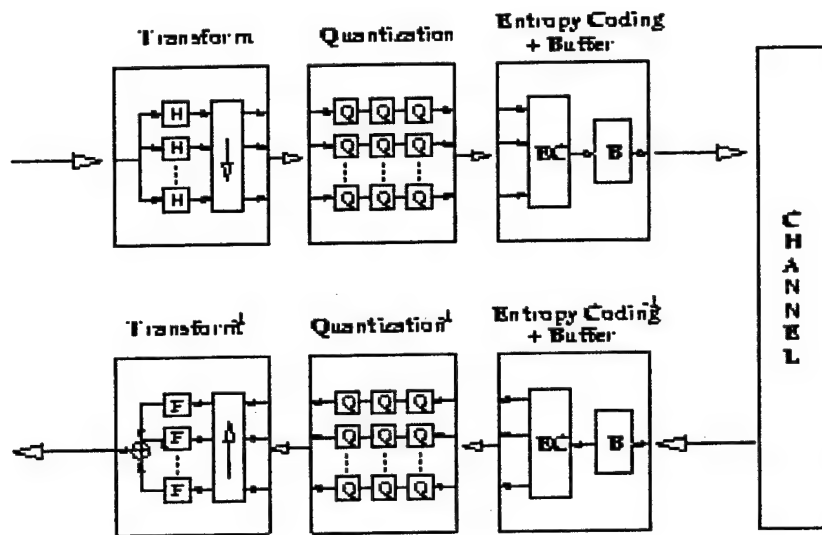


Figure 7. Block diagram of SB-RSQ system

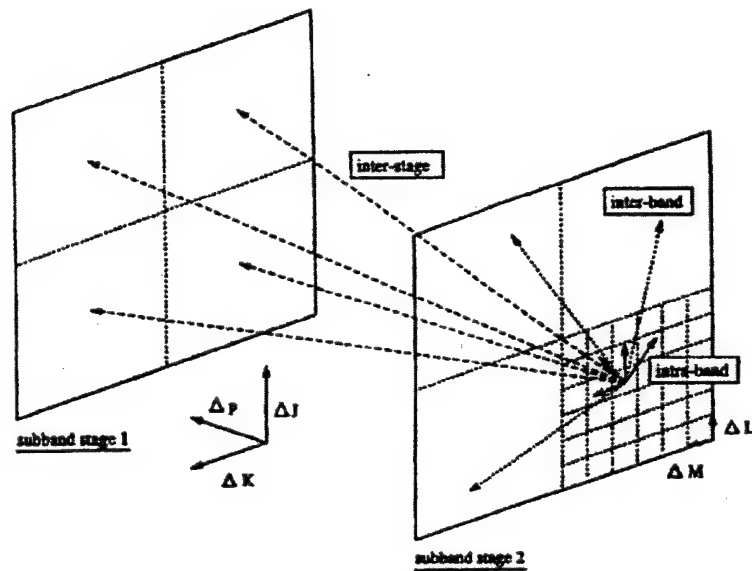


Figure 8. Diagram of the inter-stage, inter-band, and intra-band conditioning scheme

3.4.2 ERROR RESILIENT SUBBAND CODER

The error resilient algorithm developed encodes subband pixels by performing a sequence of passes in which dominant pixels are identified and coded at the bit plane level. The dominant pass consists of two tests: the node test (NT) and the descendant test (DT).

The NT of the error resilient algorithm is structured so that it produces fixed length (FL) codes. Instead of generating the bit 0 for an insignificant pixel, our NT generates the bits 00 for a positive insignificant pixel and the bits 01 for a negative insignificant pixel. Moreover, this pixel will not be tested again, as it will henceforth be considered significant. This re-structuring simplifies the entire coding structure, since each pixel in the LIP is tested exactly once by the NT and can only be refined in subsequent passes.

The DT results are variable length (VL) encoded. One bit 0 is emitted if all descendants of the subject node are insignificant while 2-3 bits are emitted otherwise. Most images have a substantial portion of their energy concentrated in the lowest frequency band. Thus, if a spatial orientation tree contains significant pixels, it is more likely that such pixels will be found at the root. As the above VL coding method spares one bit to convey this likely event, only a few bits are usually needed to code the DT results.

After completing the node and descendant tests, we perform a second pass, where each significant pixel is refined. The refinement output bits, like the NT results, are FL coded. Thus, the algorithm produces three different bit subsequences: (1) the NT subsequence representing the FL coded NT output, (2) the DT subsequence representing the VL coded significance map, and (3) the refinement subsequence. These subsequences are then protected with individualized error correcting codes. Experimental results show that this coder achieves comparable performance to standard coders like Set Partitioning in Hierarchical Trees (SPHIT) in noise-less environments, and dramatically superior results in noisy channel cases.

3.4.3 BIORTHOGONAL WAVELET CODER

Wavelet transforms have received significant attention recently due to their suitability for a number of important signal and image processing tasks, including image coding. The principle behind the wavelet transform is to hierarchically decompose the input signals into a series of successively lower resolution reference signals and their associated detail signals. At each level, the reference signals and detailed signals contain the information needed for reconstruction back to the next higher resolution level. One-dimensional DWT (1-D DWT) processing can be described in terms of a filter bank, wherein an input signal is analyzed in both low and high frequency bands. A separable two-dimensional DWT process is a straightforward extension of 1-D DWT. Specifically, in the 2-D DWT process, separable filter banks are applied first horizontally and then vertically. Application of a filter bank comprising two filters, first horizontally then vertically, gives rise to an analysis in four frequency bands: horizontal low - vertical low; horizontal low - vertical high; horizontal high - vertical low; and horizontal high - vertical high. Each resulting band is encoded according to its own statistics for transmission from a coding station to a receiving station. However, constraints exist on how filters can be designed and/or selected, including the need to output perfect reconstruction, the finite-length of the filters and a regularity requirement that the iterated low pass filters involve convergence to continuous functions. Inverse discrete wavelet transform (IDWT) can be implemented by operating DWT backwards. Interpolation operation in IDWT is used instead of decimation operation in DWT. Before the WT coefficients are transmitted, the values close to zeros (most of them are the high frequency data) can be eliminated.

Biorthogonal wavelets are attractive due to their symmetry and hence reduced computational requirement. This allows decimation of the data during the transform and reduces the number of computations. There are three components in this encoder/decoder compression model. First, the image is processed by 4-level DWT, then the WT coefficients are quantized to integers (0~255 or -128~127). Finally, Huffman and run-length coding compression is a statistical data compression technique that gives a reduction in the average code length used to represent the quantized wavelet coefficients.

4.0 RESULTS AND DISCUSSIONS

4.1 PERFORMANCE EVALUATION

Inherent with image compression is the quality of the imagery. There are long lists of mathematical metrics that have been developed to try to access the quality of an image. Some of the more common metrics that have been used for still frame imagery are mean square error (MSE), signal-to-noise (SNR), normalized SNR, and just noticeable difference (JND). Other approaches will let human observers evaluate the quality of the imagery. One well-known example of this measure is the National Imagery Interpretation Rating System (NIIRS) that has been developed by the intelligence community. While these are just a few of the performance measures, one must use these performance measures with caution and consider what the end use of the imagery will be. A representative performance measure for our Biorthogonal Wavelet and Joint Source/Channel Subband compared to the industry standard JPEG is shown in Figure 9. As an example of the image compression performance, two images are shown in Figures 11. These images show the original pentagon image (top) and the same image compressed 64:1 (bottom). The 64:1 compression shows very little loss in information content.

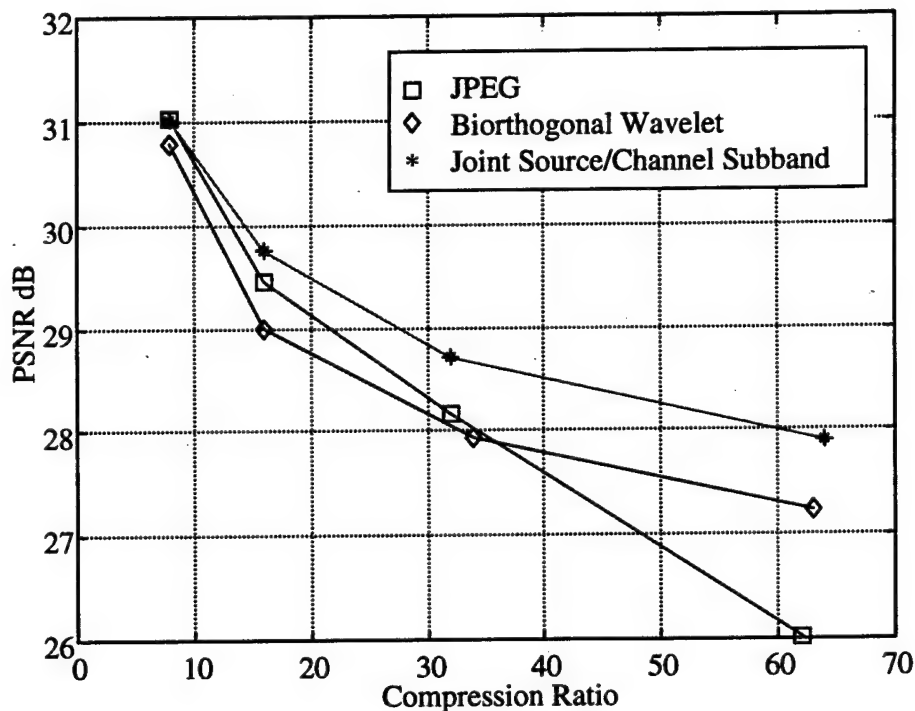
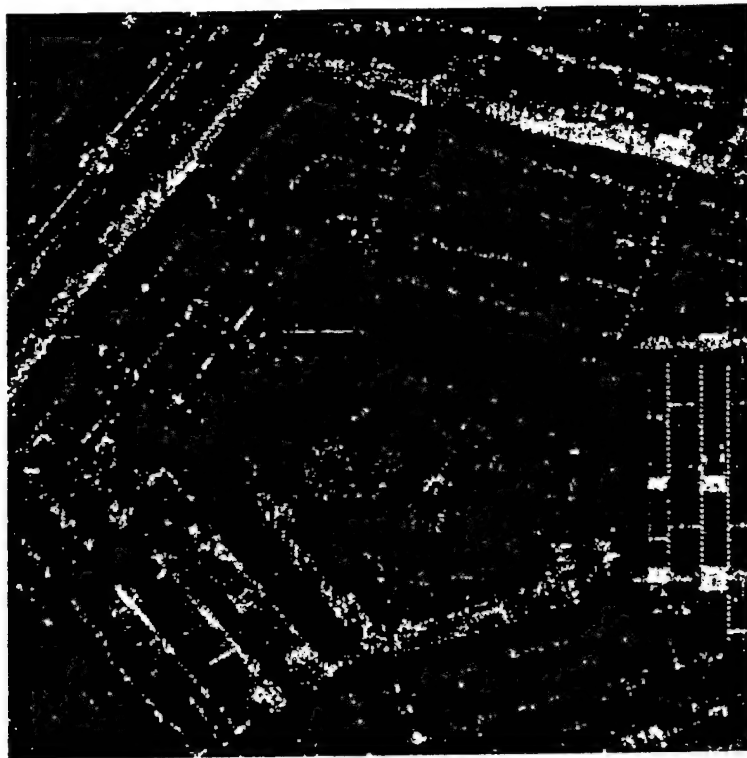


Figure 9: Performance Comparisons

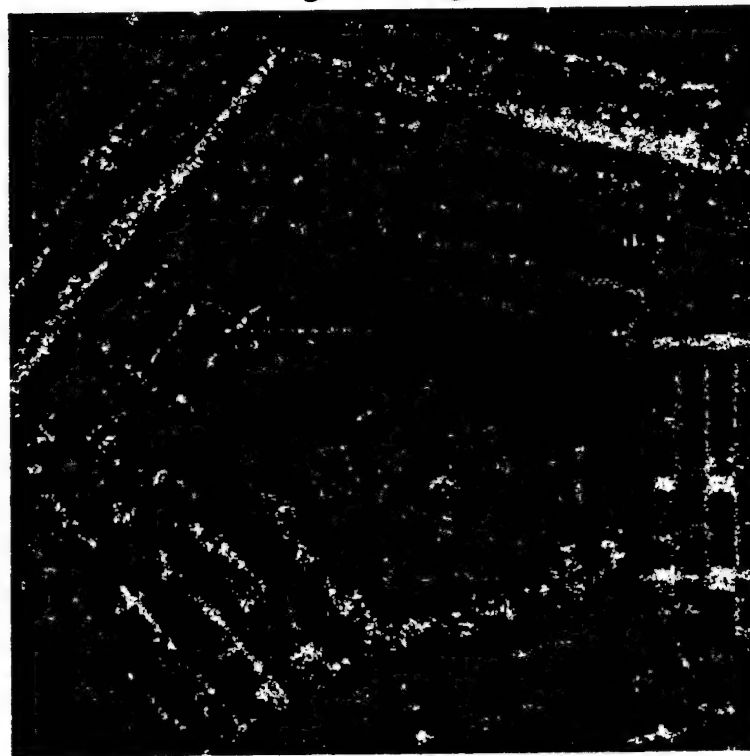
We also conducted an informal human perception test with image analysts to evaluate the imagery from military trained observers. This test was conducted using the classified Joint STARS imagery at the Trident Systems, Inc. facility in Fairfax. Trident Systems, Inc. consulted

Stephen Lee and Barry Treul from Scientific Applications International Corporation located in McLean, Virginia for these tests.

While, there was not a statistically significant amount of imagery, they were able make determinations with regards to the military utility of the imagery. For compression ratios between 10 – 20:1 using the Joint/Source/Channel Subband coder, there was little to no loss on information content. This would equate ~0.5 NIIRS or less. This would be the kind of imagery desired by imagery analysts at a primary exploitation facility. Even at the higher compression ratios of 64:1 shown in figure 10, the imagery quality was still described at high quality with less than 1 NIIRS and in some cases less than 0.5 NIIRS degradation. A more detailed discussion is described below.



Original Image



Compressed 64:1 Image

Figure 10: Image Comparisons

As reconnaissance evolved in the 1970's, physical measures such as scale and resolution no longer adequately defined the performance of imaging systems. A perceptually based measure of interpretability was developed called the National Imagery Interpretability Rating Scale (NIIRS). The initial NIIRS was developed for use with the visible spectrum imagery. The first version of NIIRS was published as a Standard NATO Agreement (STANAG) but was called the Imagery Interpretability Rating Scale (IIRS). The IIRS is no longer considered valid and has been replaced by an updated version of NIIRS that addresses visible, infrared, SAR and multispectral types of sensors. It should be noted that there are both civilian and military (intelligence) versions of NIIRS. The military version is a scale used primarily by the intelligence community as a measure that is used by imagery analysts (IA) to perform quantitative judgments on the interpretability of a particular image. The process of "rating" an image corresponds to the assignments of a number that describes the image interpretability. The NIIRS rating has been developed to ensure that imagery collection and exploitation meets the informational needs of the end user. The NIIRS is a scale from 0 to 9 that can be used to compare the products of different imaging systems. The scale has become an important tool for defining image requirements, selecting and tasking imaging systems, providing quality control feedback to operation systems and specifying performance of new imaging.

The NIIRS is defined by a set of exploitation tasks or criteria equally space across a psychophysically defined quality or interpretability scale. The NIIRS rating of an image lower valued NIIRS tasks can also be performed on the image. A NIIRS rating accounts for all of the factors affecting interpretability including resolution and sensitivity.

RADAR NIIRS (Unclassified)	
RATING	DESCRIPTION
NIIRS 0	Interpretability of the imagery is precluded by obscuration, degradation, or very poor resolution.
NIIRS 1	Detect the presence of aircraft dispersal parking areas. Detect a large cleared swath in a densely wooded area. Detect, based on presence of piers and warehouses, a port facility. Detect lines of transportation (either road or rail), but do not distinguish between.
NIIRS 2	Detect the presence of large (e.g., BLACKJACK, CAMBER, 707, 747) bombers or transports. Identify large phased-array radars by type. Detect a military installation by building pattern and site configuration. Detect road pattern, fence and hardstand configuration at SSM launch sites (missile silos, launch control silos) within a known ICBM complex. Detect large non-combatant ships (e.g., freighters or tankers) Identify athletic stadiums.
NIIRS 3	Detect medium-sized aircraft (e.g., FENCER, FLANKER, CURL, F-15). Identify an ORBITA site on the basis of a 12-meter dish antenna normally mounted on a circular building. Detect vehicle revetments at a ground forces facility. Detect vehicles/pieces of equipment at a SAM OR SSM fixed missile site. Determine the location of the superstructure (e.g., fore, amidships, aft) on a medium-sized freighter. Identify a medium-sized (approx. six track) railroad classification yard.
NIIRS 4	Distinguish between large rotary-wing and medium fixed-wing aircraft (e.g.,

	<p>HALO helicopter vs. CRUSTY transport).</p> <p>Detect recent cable scars between facilities or command posts.</p> <p>Detect individual vehicles in a row at a known motor pool.</p> <p>Distinguish between open and closed sliding roof areas on a single bay garage at a mobile missile base.</p> <p>Identify square bow shape of ROPUCHA class (LST).</p>
NIIRS 5	<p>Count all medium helicopters (e.g., HIND, HIP, HAZE, HOUND, WASP).</p> <p>Detect deployed TWIN EAR antenna.</p> <p>Distinguish between river crossing equipment and medium/heavy-armored vehicles by size and shape (e.g., MTU-20 vs. T-62 MBT).</p> <p>Detect missile support equipment at an SS-25 RTP (e.g., TEL, MSV).</p> <p>Distinguish bow shape and length/width differences of SSNs.</p> <p>Detect the break between railcars (count railcars).</p>
NIIRS 6	<p>Distinguish between variable and fixed-wing fighter aircraft (e.g., FENCER vs. FLANKER).</p> <p>Distinguish between the BAR LOCK and SIDE NET antennas at a BAR LOCK/SIDE NET acquisition radar site.</p> <p>Distinguish between small support vehicles (e.g., UAZ-69, UAZ-469) and tanks (e.g., T-72, T-80).</p> <p>Identify SS-24 launch triplet at a known location.</p> <p>Distinguish between the raised helicopter deck on a KRESTA II (CG) and the helicopter deck with main deck on a KRESTA I (CG).</p> <p>Identify a vessel by class when singly deployed (e.g., YANKEE I, DELTA I, KRIVAKII FFG).</p>
NIIRS 7	<p>Identify small fighter aircraft by type (e.g., FISHBED, FITTER, FLOGGER).</p> <p>Distinguish between electronics van trailers (without tractor) and van trucks in garrison.</p> <p>Distinguish, by size and configuration, between a turreted, tracked APC and a medium tank (e.g., BMP-1/2 vs. T-64).</p> <p>Detect a missile on the launcher in an SA-2 launch revetment.</p> <p>Distinguish between bow mounted missile system on KRIVAKI/II and bow mounted gun turret on KRIVAK III.</p>
NIIRS 8	<p>Distinguish the fuselage difference between a HIND and a HIP helicopter.</p> <p>Distinguish between the FAN SONG missile control radar and the FAN SONG F based on the number of parabolic dish antennas (three vs. one)</p> <p>Identify the SA-6 transloader when other SA-6 equipment is present.</p> <p>Distinguish limber hole shape and configuration differences between DELTA I and YANKEE I (SSBNs).</p> <p>Identify the dome/vent pattern on rail tank cars.</p>
NIIRS 9	<p>Detect major modifications to large aircraft (e.g., Airings, pods, wingless). Identify the shape of antennas on EW/GCI/ACQ radars as parabolic, parabolic with clipped corners, or rectangular.</p> <p>Identify, based on presence or absence of turret, size of gun tube, and chassis configuration, wheeled or tracked APCs by type (e.g., BTR-80, BMP-1/2, MT-LB, M113).</p> <p>Identify the forward fins on an SA-3 missile.</p> <p>Identify individual hatch covers of vertically launched SAM-6 surface-to-air system.</p>

Table 1. NIIRS Ratings Description

4.1.1 OPTIMIZED SUBBAND CODER RESULTS

The images below show the results of the optimized subband coder. Notice how the high frequency speckle is lost as the compression increases. This codec could be used for military personnel in the field that need to know quick location of enemy position. An analyst who requires speckle retention might not tolerate these images at high compression. These codecs, can provide the user with the data needed, just by adding or subtracting specific stages to the processing.

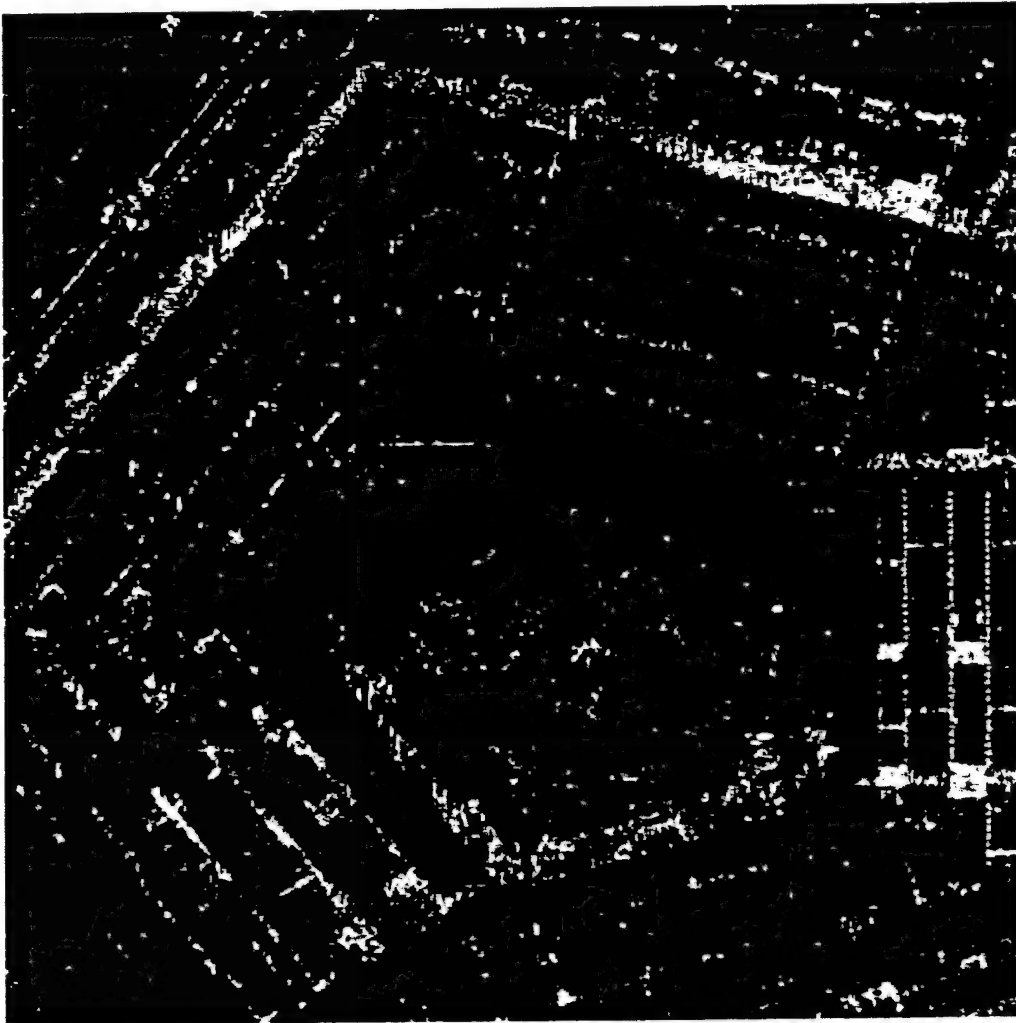


Figure 11. Pentagon Compressed 8:1 With Optimized Subband Coder

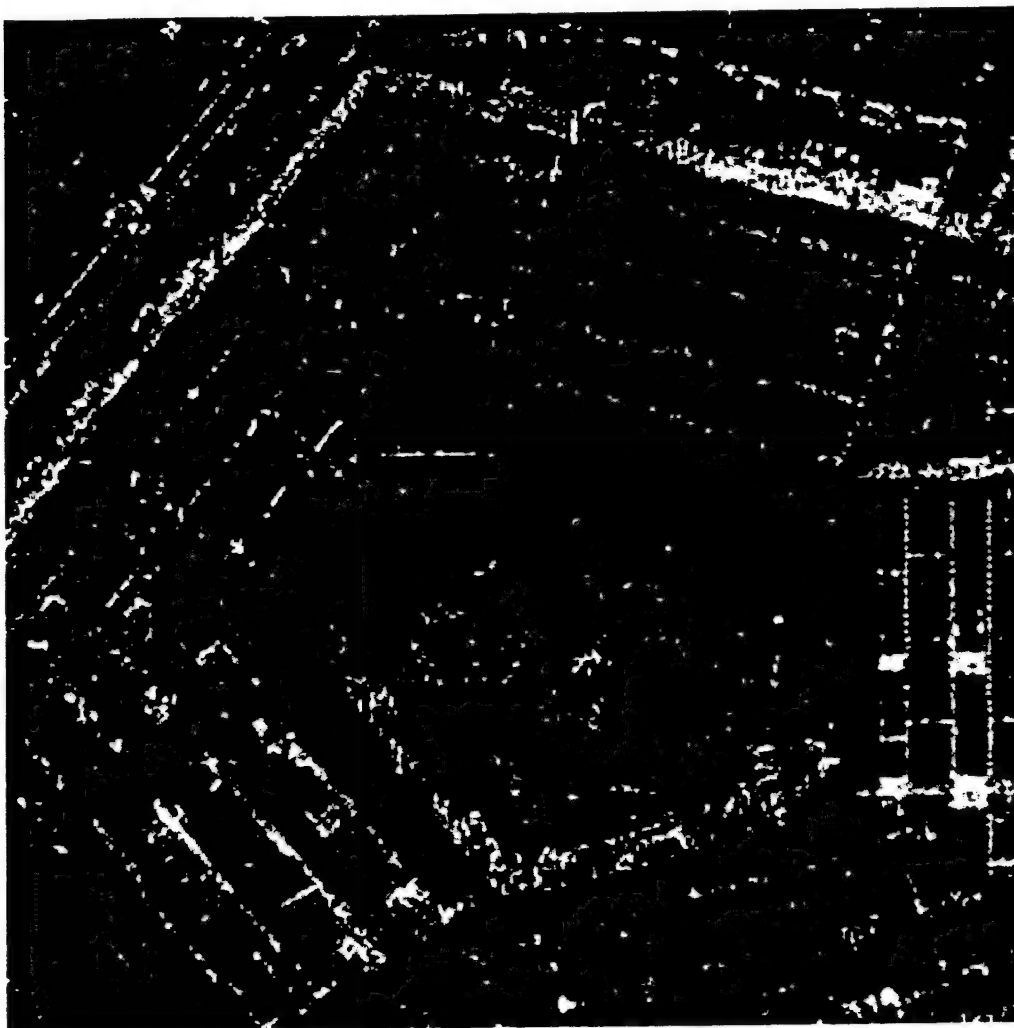


Figure 12. Pentagon Compressed 16:1 With Optimized Subband Coder

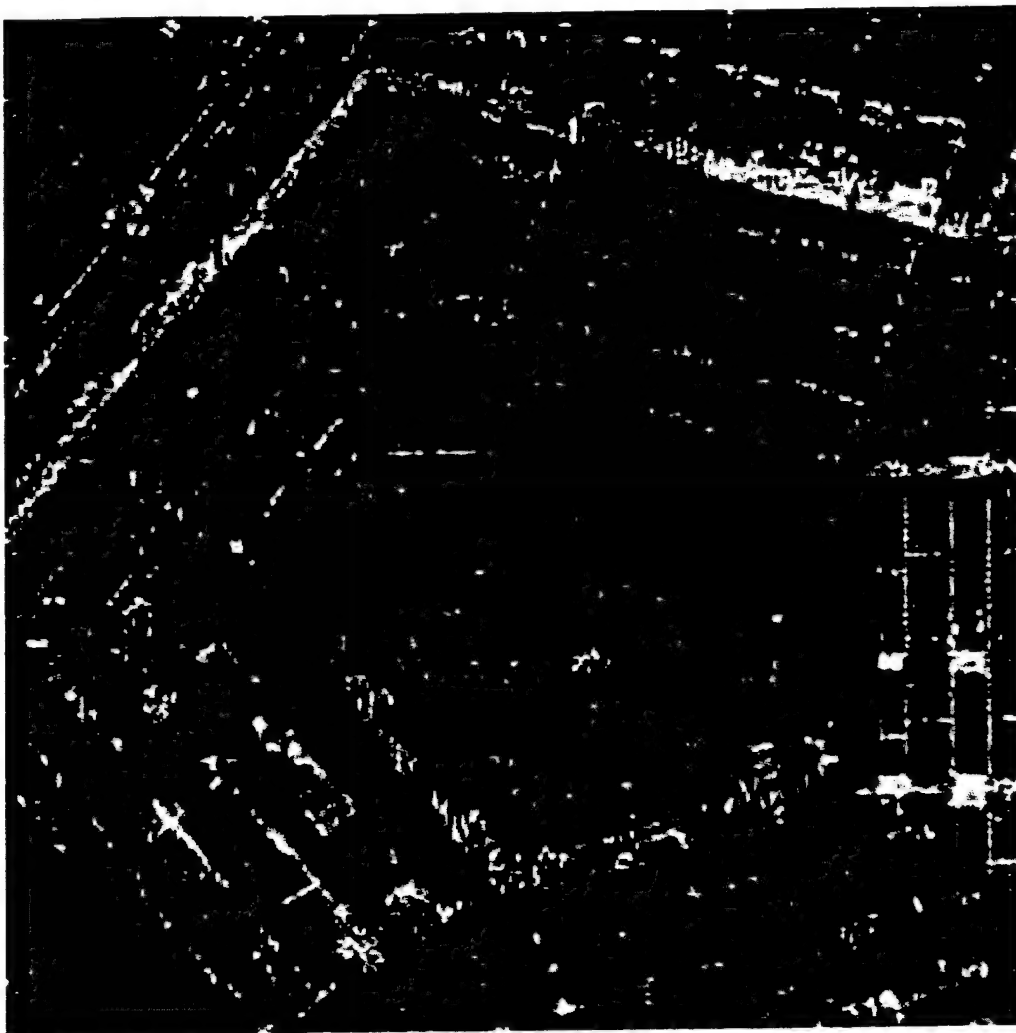


Figure 13. Pentagon Compressed 32:1 With Optimized Subband Coder

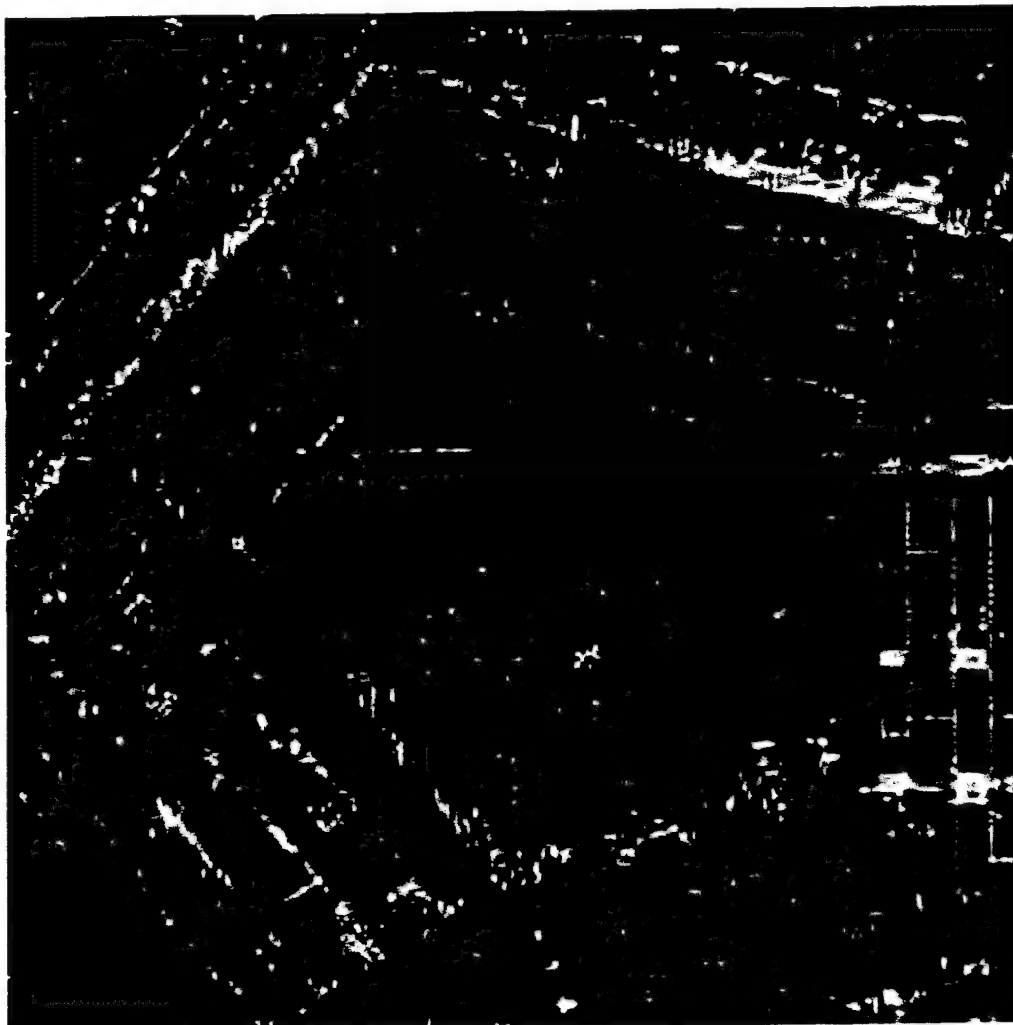


Figure 14. Pentagon Compressed 64:1 With Optimized Subband Coder

4.1.2 STRUCTURE-TEXTURE CODER RESULTS

This technique is able to give the best performance results at low bit rates among all the techniques we have tested to date. Computing PSNR, or other values such as mean square error are useless when trying to evaluate the effectiveness of this particular coder. This is due to the random speckle generation. This random speckle is similar to the original statistically, but it is not an exact replication of the speckle. Therefore, when comparing the image to the original, the generated speckle will not match the original speckle in location. However, when a system generates a SAR image of the same scene, the speckle on two images of the same scene will not match. This is important to understand when judging speckle preserving SAR compression codecs.

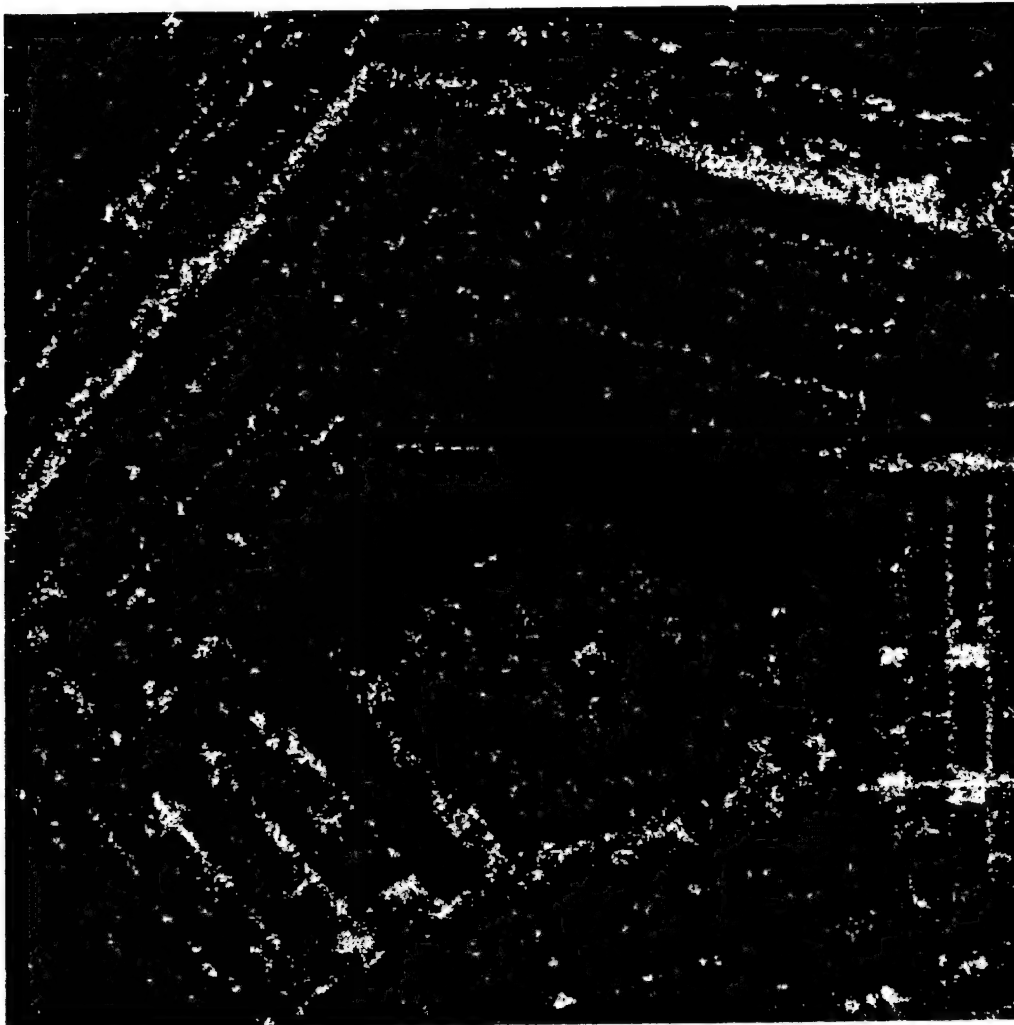


Figure 15. Pentagon Compressed 8:1 With Structure Texture Model

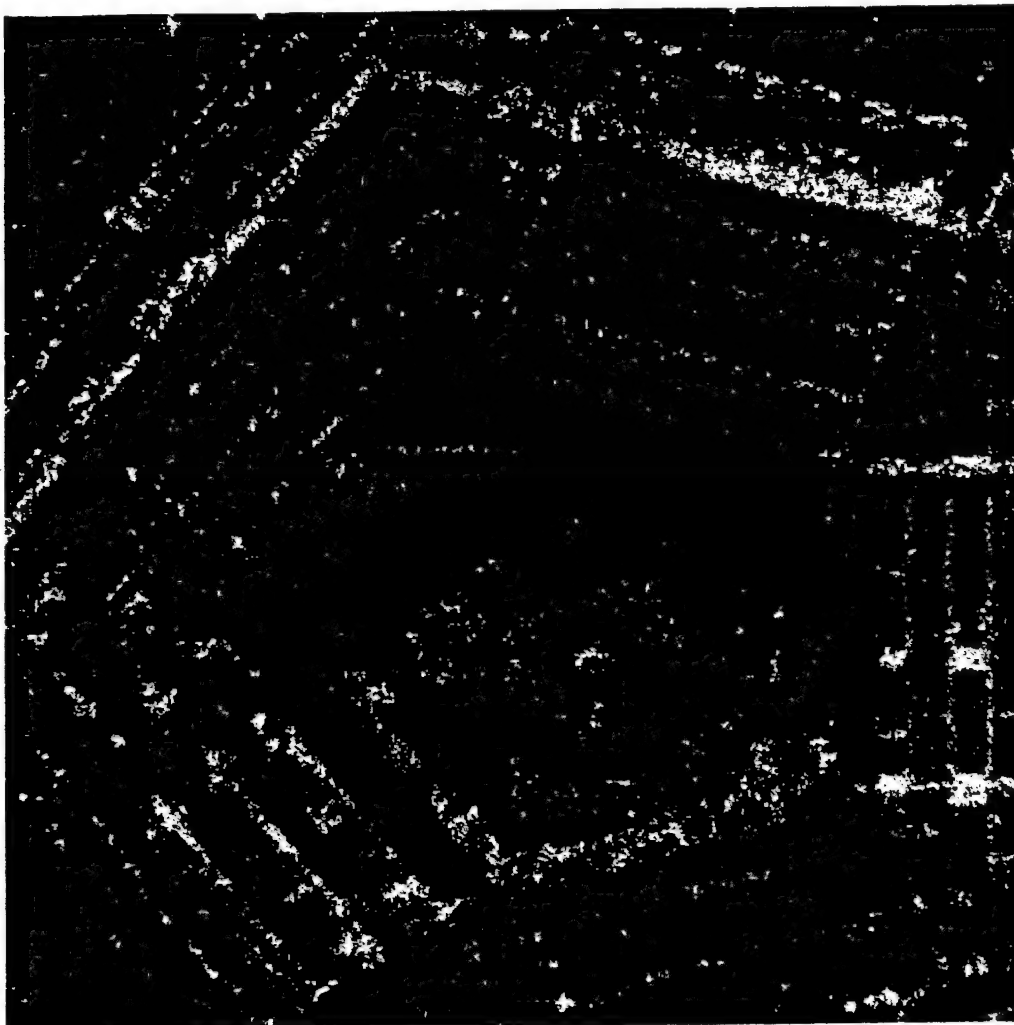


Figure 16. Pentagon Compressed 16:1 With Structure Texture Model

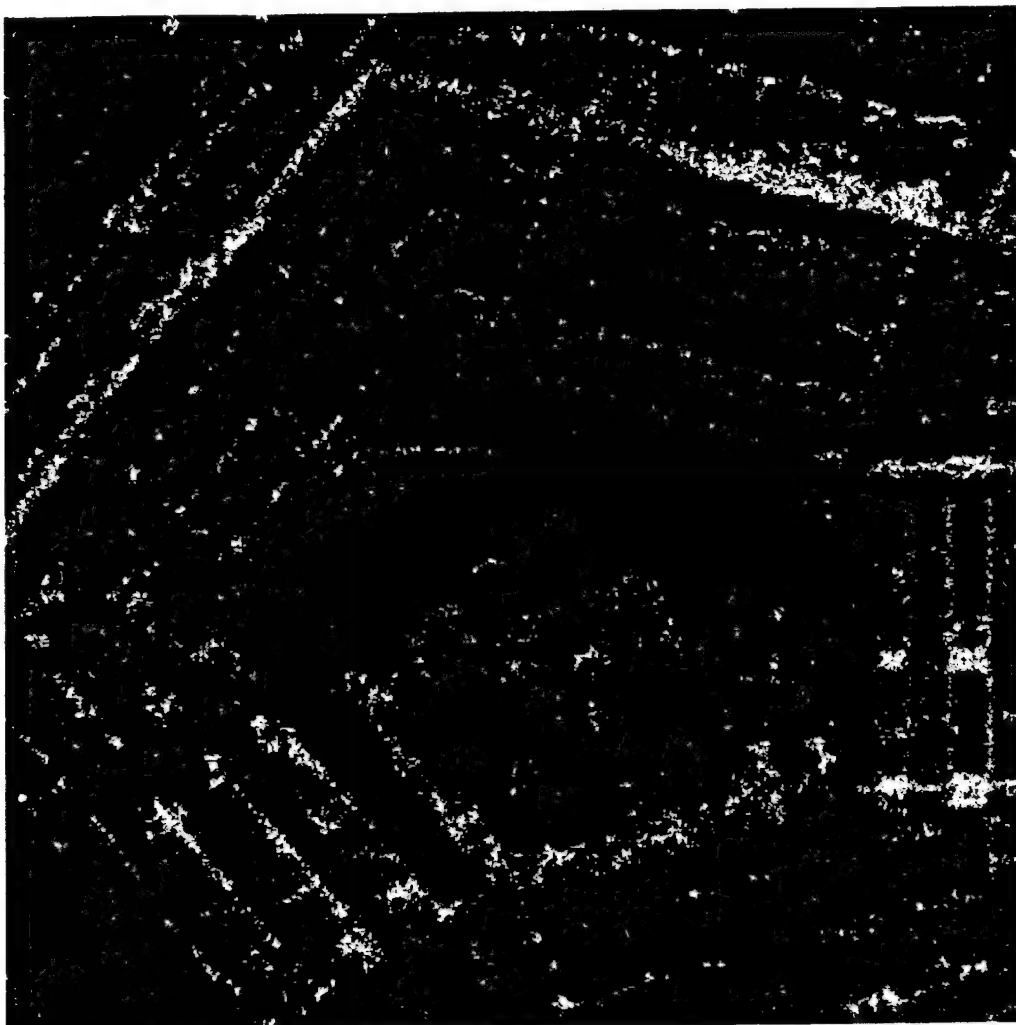


Figure 17. Pentagon Compressed 32:1 With Structure Texture Model

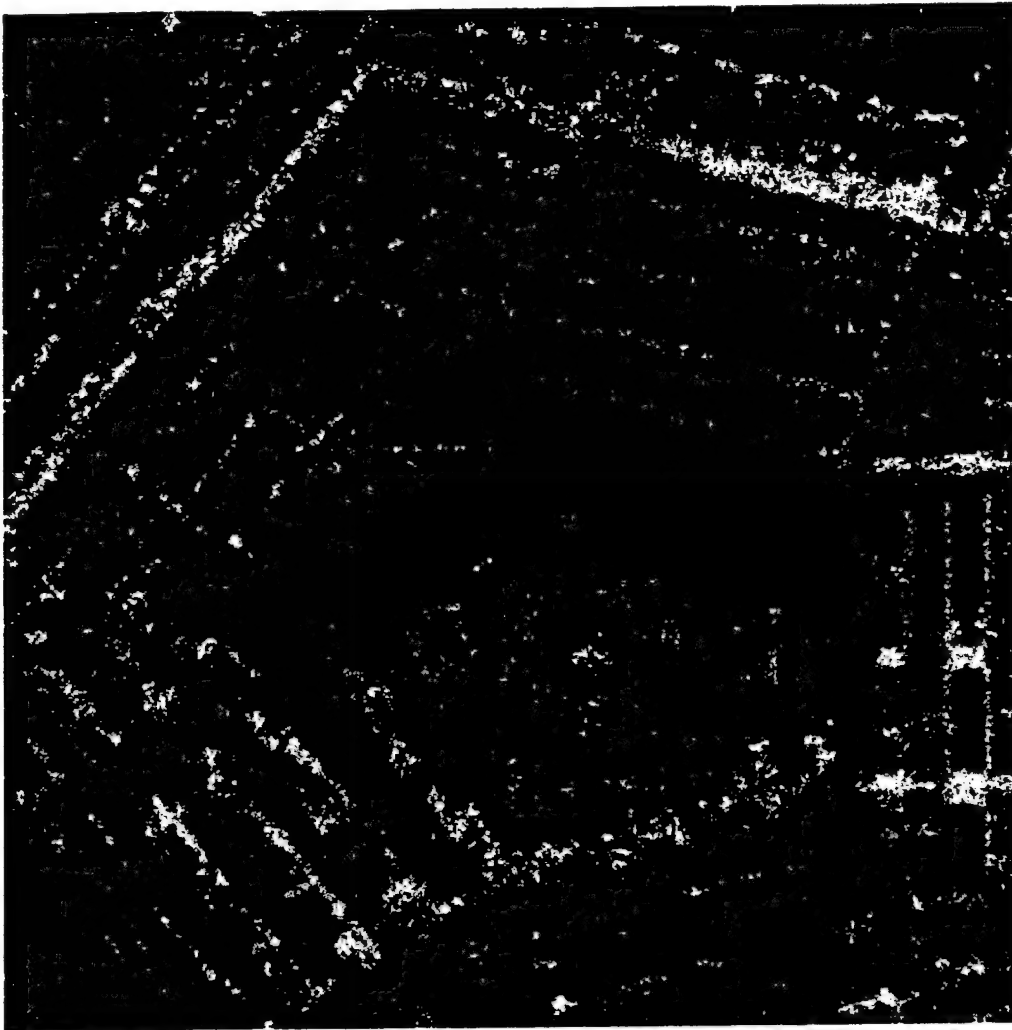


Figure 18. Pentagon Compressed 64:1 With Structure Texture Model

4.1.3 ERROR RESILIENT SUBBAND CODER RESULTS

Another important performance factor for compression systems, is their robustness against channel errors. Most compression algorithm developers strive to achieve the best compression performance without regard to what will happen in the real world environment with very noisy military communication systems. This system can have bit error rates as high as 10^{-1} . While there are a number of very good compression algorithms, often a single bit error can cause severely degrade the reconstructed image and in some cases render the image totally useless.

As an example several images are shown in the section below. The first image is the original, the second image is compressed to 0.25 bpp with a BER of 10^{-4} using the zero tree algorithm of Said and Pearlman (SPHIT), and the third image is compressed with our error resilient subband coder.

The SPHIT image shows significant distortion especially around the targets and in uniform areas while our error resilient approach does not exhibit these distortions.

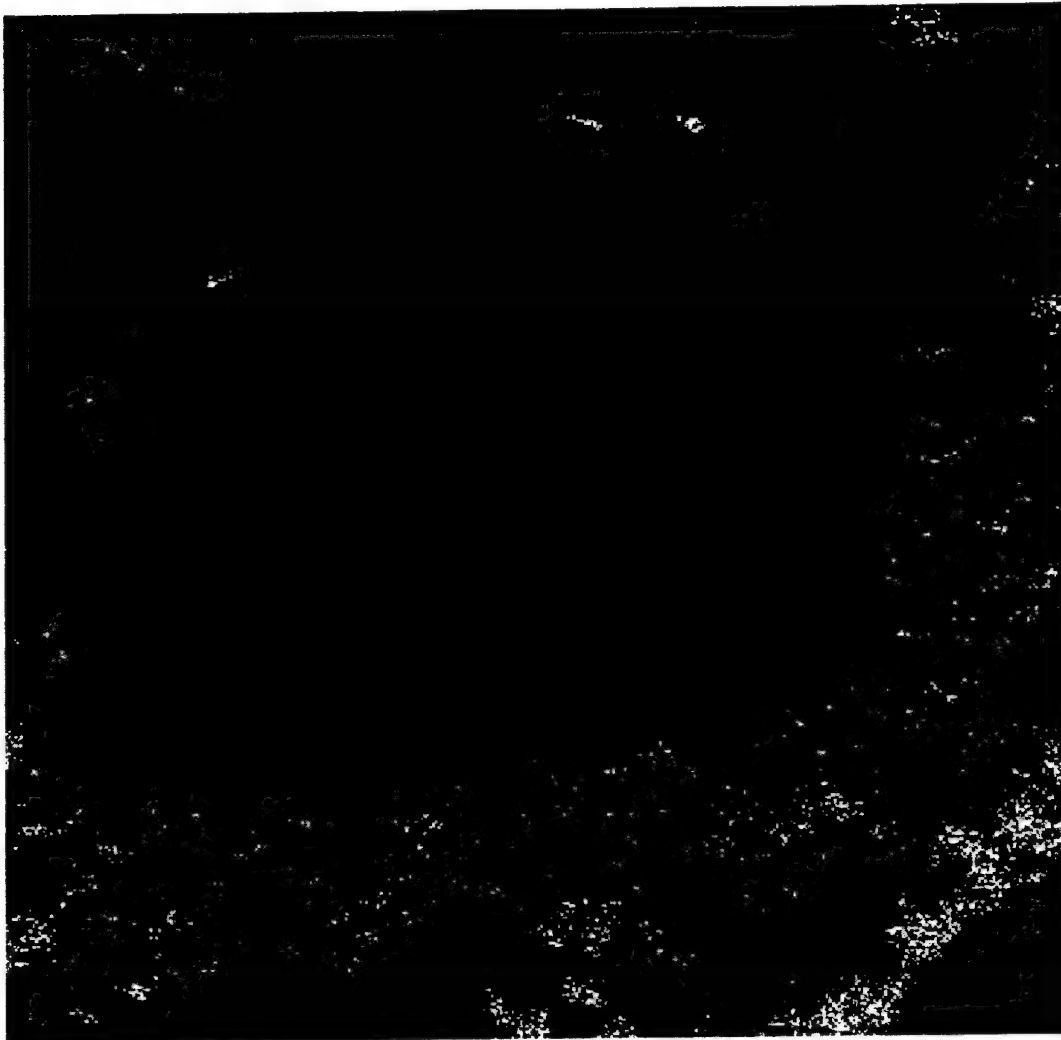


Figure 19. Original Image

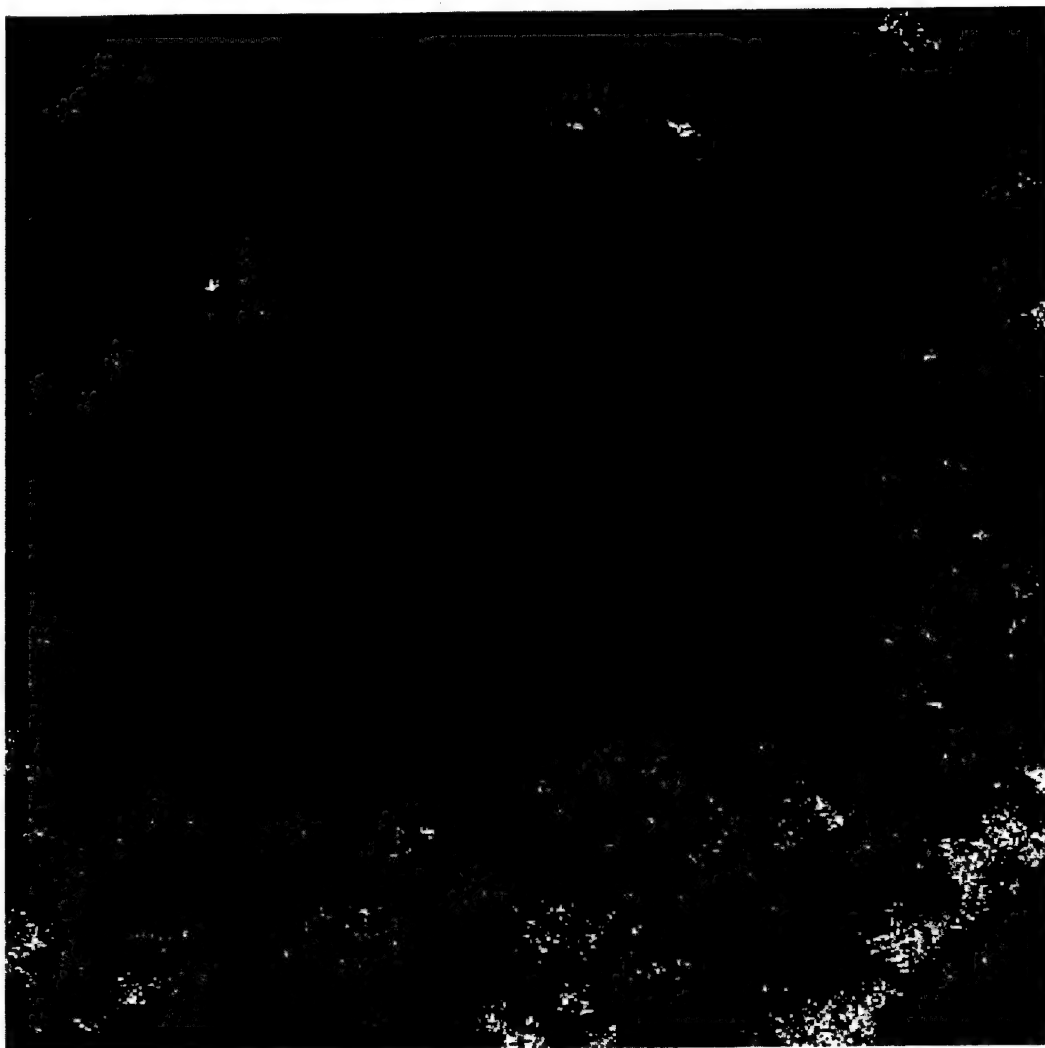


Figure 20. SPHIT Image Compressed to 0.25 bpp With a BER of 10^{-4}

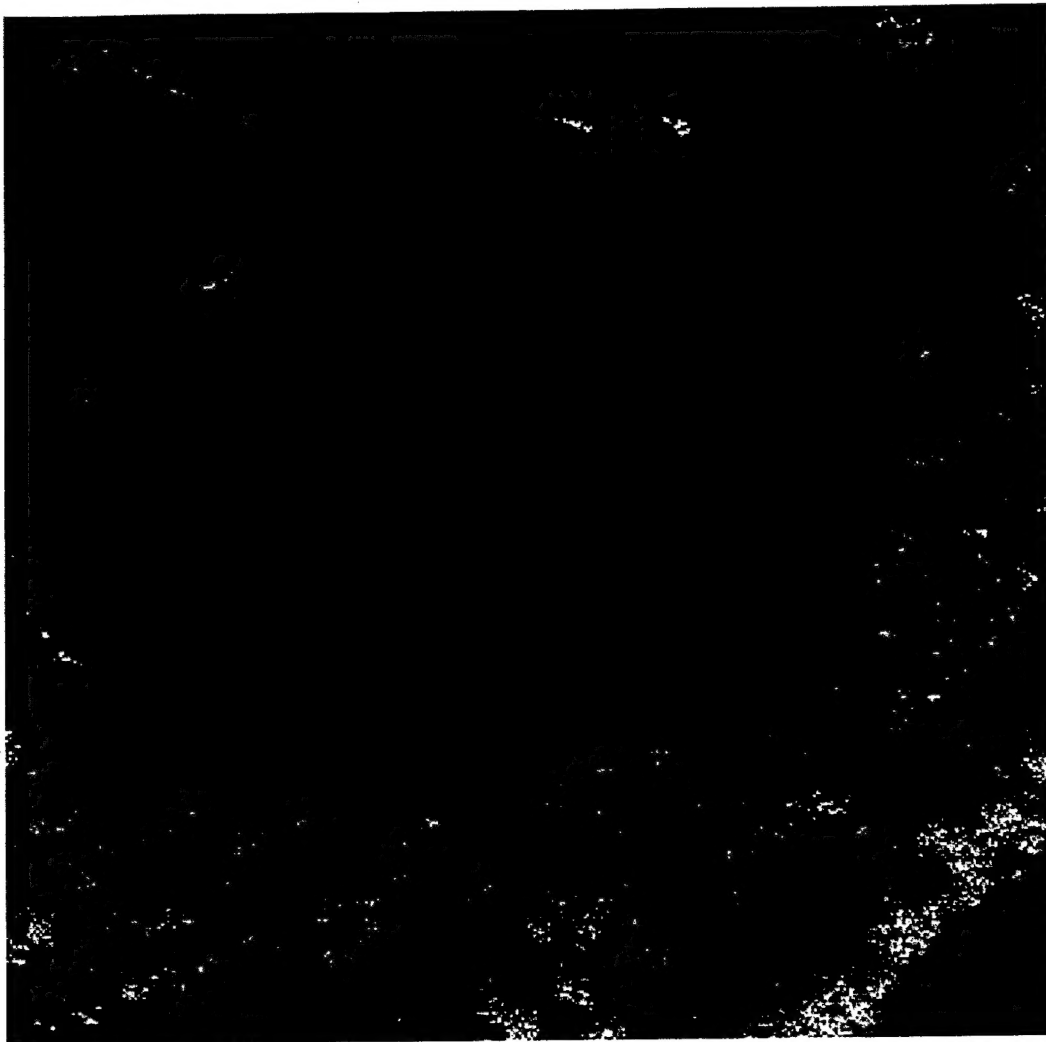


Figure 21. Error Resilient Image Compressed to 0.25 bpp With a BER of 10^{-4}

5.0 CONCLUSIONS

There are many needs for imagery on the battlefield. However, the needs of individuals on the battlefield differ. Some may need to simply know the location of enemy equipment, while others may need to know the exact type of that equipment and information about the surrounding area. This requires different levels of detail in the image. That is why image compression, and the quality of the compressed imagery is such an objective evaluation.

As far as visual appearance of compressed imagery, our Structure Texture codec is the best combination of our processing and compression models. It is able to separate the speckle from the image, without destroying much of the edge information found in that image. The structure and speckle are then compressed separately. This allows the structure part of the image to be compressed at different levels, without the loss of speckle. Our image experts confirmed our evaluation of codecs, and determined that the sample test joint STARS images compressed 64:1 with our structure texture codec provided very good results. On most images of our test set, the analysts noticed less than a step of NIIRS degradation.

Many of the military communications systems, especially at the tactical level, have very narrow bandwidths (typically less than 16 Kbps) and transmitting large amounts of data is a very time consuming process. An 8 bit image that is 1000 x 1000 pixels transmitted over a 16 Kbps link would take over 8 minutes to complete. Using our structure texture model would allow transmission over the standard communications system, in only eight seconds and would provide essentially the same information to the end user.

The structure texture model has the highest computational requirements of all our models. This is extremely evident in the speckle regeneration.

If speckle is not important to the end user, either the biorthogonal wavelet coder, or the optimized subband coder could perform adequately for the user. Also, these coders combined with the pre and post processor could allow for even higher compression while yielding images acceptable to a user that does not require the finest detail in the images. As with all codecs, quality is increased with the addition of more data.

6.0 FUTURE CONSIDERATIONS

The Phase II effort will continue the development and evaluation SAR compression and enhancement algorithms for Joint STARS that will achieve the highest compression ratio while still maintaining high image quality, preservation of image detail and being computationally efficient. Closely coupled with this algorithm development will be the close working relationship with the Joint STARS program (both the prime contractor and the government) to ensure that the algorithm approach will meet the end users requirements.

The algorithms that have been developed during the Phase I effort have shown very good performance when compared to other state of the art approaches. For the Phase II effort, we will continue to refine and enhance our algorithm suite in order to further improve on our accomplishments. We will also evaluate our compression algorithm approach with the JP2000 algorithm as it becomes finalized. It should be noted that our team is a member of the JPEG2000 working group and is submitting an algorithm for evaluation. We will also evaluate our enhancement algorithms (pre/post and structured/textured) with the JPEG2000 algorithm.

The main focus on the algorithm development will be to explore the integration of the best features of each of the algorithms. This includes the error resilience coder and the optimized subband that should provide a coder with higher performance and robustness to channel noise. Further optimization can further be achieved by focusing on the specific SAR resolution.

While all of the initial algorithm development work will be done in MATLAB, the final software prototype will be designed for the targeted processor system for the upgrade signal processor for Joint STARS. The upgraded processor for Joint STARS is based on the Multiport heterogeneous architecture from Mercury Computer Systems which includes PowerPC RISC processors and SHARC digital signal processors (from Analog Devices) integrated via Mercury's RACEway interconnect.

7.0 REFERENCES

1. Harold Szu, Charles Hsu, Joseph Landa, Terry Jones, Barbara O'Kane, John O'Connor, Romain Murenzi, and Mark Smith, "Image Compression Quality Metrics," Proceedings of SPIE AeroSense 97.